LOW-COST PIEZOELECTRIC ACTUATORS – ANALYTICAL, NUMERICAL AND EXPERIMENTAL STUDIES WITH A FOCUS ON MOBILE ROBOTICS

Felix Becker[1], Simon Börner[1], Emmanuel James[1], Vladimir Minchenya[2], Klaus Zimmermann[1]

[1]Technische Universität Ilmenau, Technical Mechanics Group
[2]Belarusian National Technical University Minsk, Department of Construction and
Production of Instruments

ABSTRACT

In this paper we discuss the static and dynamic behaviour of low-cost piezoelectric circular unimorph actuators with the aim to use them as a vibration motor for miniaturized mobile robots. The discussed example consists of two layers: a brass plate and a piezoelectric ceramic layer. For the analytical description, the actuation system is modelled as a thin elastic plate, which can be described with the help of the Kirchhoff hypothesis of plates and laminates. For the numerical analysis, a finite element model was created and solved using the program package ANSYS®. The results are compared with measurements using a scanning laser vibrometer. It can be concluded that the studied piezoelectric low-cost unimorphs can be used as vibration actuators in the considered frequency range, but that the static and dynamic behaviour of individual unimorphs differs considerably due to manufacturing tolerances.

Index Terms – piezo actuator, unimorph, theory of plates, micro robot

1. INTRODUCTION

Piezoelectric unimorph actuators consist of a thin layer of piezoelectric material and a passive layer, which are glued together. The study is conducted with the actuator presented in Figure 1. It is an example for similar circular unimorphs, which are available in a diameter range from 10 mm up to 50 mm. The discussed actuator consists of a brass plate and a piezoelectric ceramic layer with respective diameters of 50 mm and 30 mm and a height of 0.2 mm each. For example, such actuators are used as audio signal devices (buzzers) or as active membranes in miniaturized pumps. Because of their vibration characteristic and the low price, they can be used as vibration motors for low-cost miniaturized robots, as presented in [1] or [2]. Such robots perform locomotion due to resonant vibrations of elastic contact elements between the robot and the ground. A high frequency ($>1000\,Hz$) excitation is performed by actuators similar to the one displayed in Figure 1. Below, the index "P" points to the piezo ceramic and "M" names the metal (brass).
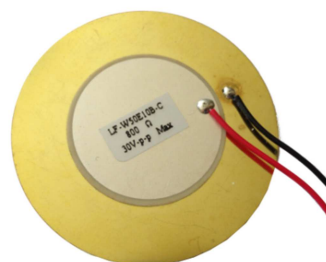

Figure 1: Low-cost piezoelectric unimorph actuator (Ø 50mm)

2. ANALYTICAL MODEL

The actuator is modelled, following [3], as a thin elastic laminate, see Figure 2, using the *Kirchhoff hypothesis of plates* [4] for laminates, which is often named *Classical theory of laminates* [5].
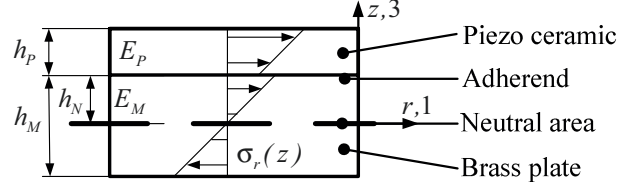

Figure 2: Laminate of two thin elastic plates

h_P and h_M are the height of the piezo and the metal layer. E_P and E_M are the Young's moduli of the materials. It is assumed that the adherend is ideal, which means that the height of it equals zero and there is no motion between the plates. The influences of the electrodes, cables and soldering points to the static deflection $w(r)$ are neglected. Furthermore it is assumed, that the piezo ceramic and the metal have approximately the same Poisson's ratio ν. For the use of the Kirchhoff hypothesis, the introduction of a strain- and stress-free area is needed. The position of the neutral area can be calculated from the condition

$$\int_z \sigma_r dz = 0 \text{, with } \sigma_r = \frac{E}{1-\nu^2}\left(w'' + \frac{\nu}{r}w'\right)z \text{.}$$

2.1 Bending stiffness

Figure 2 shows the cross section of the laminate and the radial stress distribution $\sigma_r(z)$ using cylindrical coordinates (r, φ, z). If the distance between the adherend and neutral area is h_N, it follows

$$\frac{1}{1-\nu^2}\left(w'' + \frac{\nu}{r}w'\right)\left(E_M \int_{-(h_M-h_N)}^{h_N} z\,dz + E_P \int_{h_N}^{h_N+h_P} z\,dz\right) = 0 \text{,}$$

and with the ratios of Young's moduli and heights

$$e = \frac{E_P}{E_M} \text{,} \qquad\qquad a = \frac{h_P}{h_M} \text{,}$$

the unknown h_N can be determined:

$$h_N = \frac{h_M}{2} \times \frac{1-ea^2}{1+ea} \text{.}$$

Taking into account the inner moment

$$\tilde{m}_R = \int_z \sigma_r \, z \, dz \text{,}$$

for the bending stiffness of the laminate follows

$$N_{PM} = N_0 \times \frac{4\left(1+ea^3\right)\left(1+ea\right) - 3\left(1-ea^2\right)^2}{1+ea} \text{,} \qquad (1)$$

where

$$N_0 = \frac{E_M h_M^3}{12\left(1-\nu^2\right)} \qquad (2)$$

is the bending stiffness of homogeneous metal plate of the height h_M.

2.2 Piezoelectric bending moment

The electro-mechanical properties of piezoelectric materials are determined by two field equations. For the description of the actuation effect is used

$$\vec{\varepsilon} = s^E \vec{\sigma} + d^T \vec{E}_{el}.$$

The sensing capabilities are not considered. $\vec{\varepsilon}$ is the superposition of the mechanical and electrical induced strain. s^E gives the compliance in a constant electrical field $\vec{E}_{el}$. In piezoelectric materials an applied electrical field $\vec{E}_{el}$ results in a mechanical strain, coupled by the transposed matrix of piezoelectric moduli d^T. Using a cylindrical coordinate system, neglecting shear stress and considering the electrical field in the direction of the polarization, see Figure 3 (a), the scalar equations follow:

$$\varepsilon_r = s^E_{11}\sigma_r + s^E_{12}\sigma_\varphi + s^E_{13}\sigma_z + d_{31}E_{z,el},$$
$$\varepsilon_\varphi = s^E_{12}\sigma_r + s^E_{11}\sigma_\varphi + s^E_{13}\sigma_z + d_{31}E_{z,el}, \tag{3}$$
$$\varepsilon_z = s^E_{13}\sigma_r + s^E_{13}\sigma_\varphi + s^E_{33}\sigma_z + d_{33}E_{z,el}.$$

The numerical indices follow the standardised diction of DIN EN 50324-2. For the considered problem the indices could be transformed: $1 \rightarrow r$, $2 \rightarrow \varphi$ and $3 \rightarrow z$. As the plate is sufficiently thin it can be assumed

$$\sigma_z = 0.$$

Piezoelectric materials for the considered actuators show an isotropic behaviour in the (r,φ)-plane:

$$s^E_{12} \approx -\nu s^E_{11}.$$

For the used shear effect the effective Young's modulus is

$$E_P = \frac{1}{s^E_{11}}.$$

Now (3) can be written as

$$\varepsilon_{r,P} = \frac{1}{E_P}\left(\sigma_{r,P} - \nu\sigma_{\varphi,P}\right) + d_{31}E_{z,el}, \qquad \varepsilon_{\varphi,P} = \frac{1}{E_P}\left(\sigma_{\varphi,P} - \nu\sigma_{r,P}\right) + d_{31}E_{z,el},$$

with the electrical field

$$E_{z,el} = \frac{U}{h_P}.$$

With Hooke's law

$$\sigma_r = \frac{E}{1-\nu^2}\left(\varepsilon_r + \nu\varepsilon_\varphi\right), \qquad \sigma_\varphi = \frac{E}{1-\nu^2}\left(\varepsilon_\varphi + \nu\varepsilon_r\right)$$

and the condition of the equality of length of piezo and metal layer in the interval $0 \le r \le R_P$
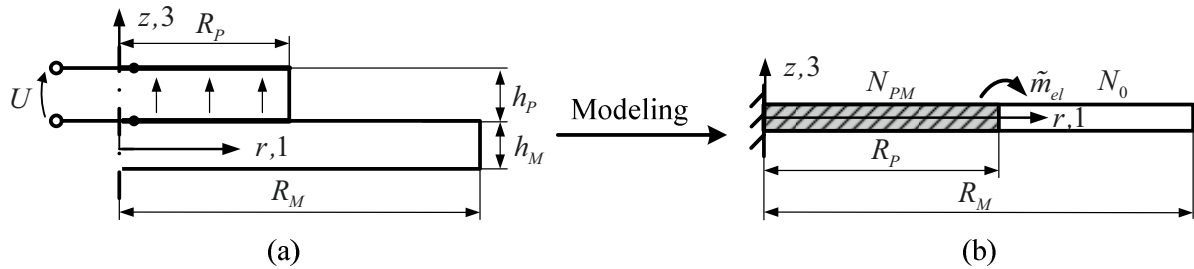
$$\sigma_{r,P}h_P + \sigma_{r,M}h_M = 0$$

Figure 3: (a) Piezoelectric actuator with direction of polarisation and applied voltage U;
(b) Mechanical model with piezoelectric bending moment

can be determined the piezoelectric bending moment

$$\tilde{m}_{el} = \int_z \sigma_r z\, dz = -d_{31} U \times \frac{E_P h_P}{1-\nu} \times \frac{1+a}{2a(1+ea^2)}. \tag{4}$$

2.3 Deflection of the actuator

Further the actuator is modelled, as presented in Figure 3 (b). It consists of a circular plate with the radius R_P and the stiffness N_{PM}, (1) , and a circular ring plate with $R_P \leq r \leq R_M$ and N_0, (2). The determined moment $\tilde{m}_{el}$, (4), is applied. The deflection of the plate is described by the Kirchhoff's plate equation

$$\Delta\Delta w = \frac{p}{N}.$$

In the considered rotationally symmetric case with

$$p = 0$$

follows for the homogeneous equation

$$\Delta\Delta w(r) = w'''' + \frac{2}{r}w''' - \frac{1}{r^2}w'' + \frac{1}{r^3}w' = 0.$$

The general solutions for the different intervals are:

$$0 \leq r \leq R_P: \quad w_P(r) = C_1 + C_2\,ln\,r + C_3 r^2 + C_4 r^2\,ln\,r,$$

$$R_P \leq r \leq R_M: \quad w_M(r) = C_5 + C_6\,ln\frac{r}{R_M} + C_7 r^2 + C_8 r^2\,ln\frac{r}{R_M}.$$

With the boundary conditions of the problem

$$w_P(0) = 0, \quad w'_P(0) = 0, \quad w_P(R_P) = w_M(R_P), \quad w'_P(R_P) = w'_M(R_P),$$

$$\tilde{q}_{r,P}(R_P) = \tilde{q}_{r,M}(R_P), \quad \tilde{m}_{r,P}(R_P) = \tilde{m}_{r,M}(R_P) + \tilde{m}_{el}, \quad \tilde{q}_{r,M}(R_M) = 0, \quad \tilde{m}_{r,M}(R_M) = 0,$$

where the shear force and the bending moment are

$$\tilde{q}_r(r) = -N\left(w''' + \frac{1}{r}w'' - \frac{1}{r^2}w'\right), \qquad \tilde{m}_r(r) = -N\left(w'' + \frac{\nu}{r}w'\right),$$

the unknown constants $C_1,..,C_8$ can be calculated. The following ratios are used:

$$e = \frac{E_P}{E_M}, \qquad a = \frac{h_P}{h_M}, \qquad \eta = \frac{N_{PM}}{N_0}, \qquad \chi = \frac{R_P}{R_M}, \qquad \kappa = \frac{1-\nu}{1+\nu}.$$

For the deflection of the piezoelectric actuator follows:

$$w(r) = \begin{cases} -\tilde{m}_{el}\dfrac{R_P^2}{2N_0(1+\nu)} \times \dfrac{1}{\eta(1+\chi^2\kappa) + \kappa(1-\chi^2)}(1+\chi^2\kappa)\dfrac{r^2}{R_P^2}; & for \quad 0 \leq r \leq R_P \\[2em] -\tilde{m}_{el}\dfrac{R_P^2}{2N_0(1+\nu)} \times \dfrac{1}{\eta(1+\chi^2\kappa) + \kappa(1-\chi^2)}\left(1 + \kappa\dfrac{r^2}{R_M^2} + 2\,ln\dfrac{r}{R_P}\right); & for \quad R_P \leq r \leq R_M. \end{cases}$$

The plot of $w(r)$ in Figure 6 was done for the following material parameters.

Table 1: Parameters of the analytic solution

		Metal (brass)		Piezo ceramic	Unit
Young's modulus	E_M	100	E_P	59.4	GPa
Density	ρ_M	8500	ρ_P	7760	kg/m^3
Poisson's ratio	ν	0.355	ν	0.355	
Piezo constant			d_{31}	-2.14×10^{-10}	m/V

3. FINITE ELEMENT MODELING

For the numerical analysis a finite element model was created and solved using the program package ANSYS® Mechanical APDL 14.5. The model consists of two types of elements: SOLID5 and SOLID186. The model is similar to the analytical and consists of two layers, which are ideal glued together by merging the layer's nodes. The actuator is fixed in the middle. The parameters of the piezoelectric material were defined as given below.

The model was used to calculate the static deflection of the actuator. As presented in Figure 6, the results agree with the plate theory and the experiments.

Table 2: Piezo material parameters of the numerical analysis

```
/com   Piezo materiel      Z-polarized


/com   Stiffness
TB,   ANEL, 1      ,      1     ,      0
TBDATA,      1,    1.0760E+11   ,      6.3129E+10   ,      6.3862E+10
TBDATA,      7,    1.0041E+11   ,      6.3862E+10
TBDATA,     12,    1.0041E+11
TBDATA,     16,    2.2237E+10
TBDATA,     19,    1.9623E+10
TBDATA,     21,    1.9623E+10


/com   Piezo matrix
TB,   PIEZ, 1
TBDATA,      3,    -9.5226
TBDATA,      6,    -9.5226
TBDATA,      9,    15.1393
TBDATA,     14,    11.9702
TBDATA,     16,    11.9702


/com   Permittivity
EMUNIT,      EPZRO, 8.85E-12
MP,   PERX, 1    ,      1111
MP,   PERY, 1    ,      1111
MP,   PERZ, 1    ,      825
/com   Density
MP,   DENS, 1    ,      7760
```

4. MEASUREMENT OF STATIC DISPLACEMENT

To compare the analytical and numerical models with the actual actuators, the static displacements of five actuators were measured. Using the measuring configuration displayed in Figure 4 a) it was possible to measure displacements with a resolution of about 1µm with an applied voltage to the piezo up to 90 V. The actuator was fixed by a steel rod orthogonally glued to the centre. This rod was mounted in a holder so the displacement of the centre was zero at all times. The *LD-1605-2* made by the *Micro-Epsilon Messtechnik GmbH & Co. KG* is an optical sensor which uses a laser beam to measure relative displacements based on triangulation. The actuators highly reflective brass surface is not suited for this sensor because the laser beam would be reflected back to its source. To achieve a diffuse reflection, small 2x2 mm² pieces of white tape were put at the measuring positions shown in Figure 4 b).
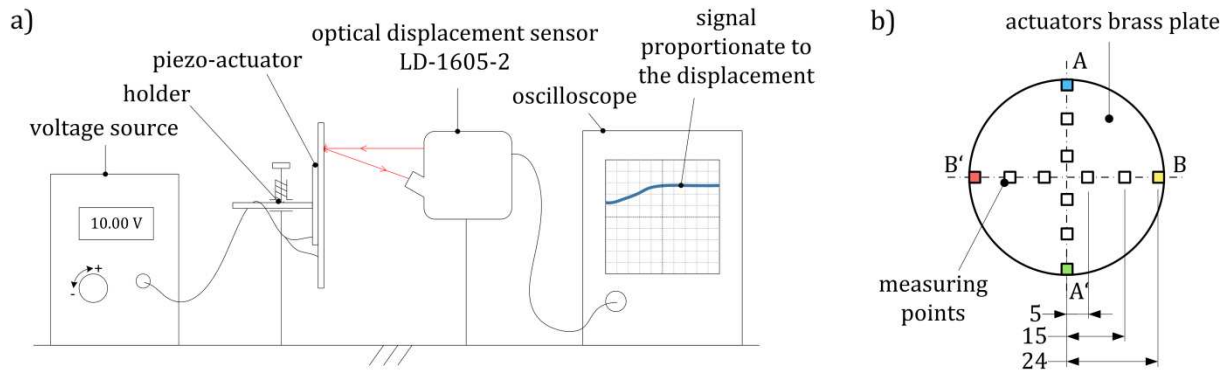
Figure 4: a) Measuring configuration, b) Positioning of measuring points on the brass surface

The static displacements of five piezoelectric actuators were measured for nine voltages ranging from 10 V to 90 V. Figure 5 shows the results for each piezo actuator at the outer measuring points with an applied potential of 90 V.
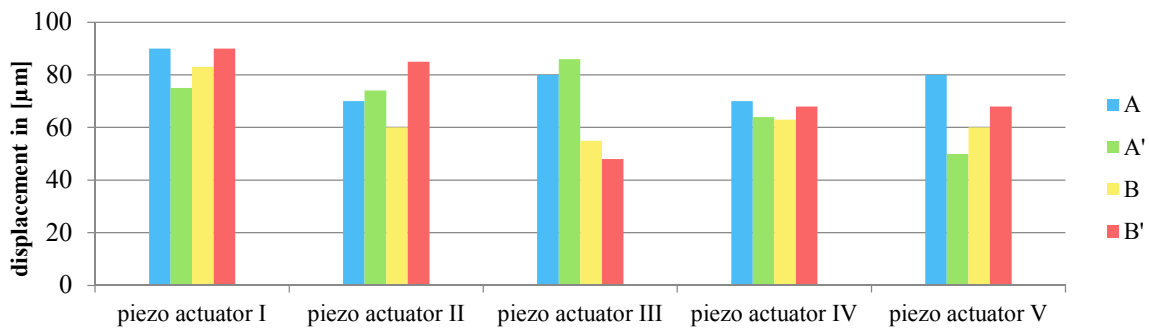
Figure 5: Displacements of five piezo actuators at the outer measuring points with an applied potential of 90 V

An ideal actuator would result in identical displacements for each measuring point. But, as shown in Figure 5, the maximum displacement differs from 48 µm to 90 µm. It can be concluded that the production tolerances for these low-cost piezoelectric unimorph actuators are rather high and that the deflection cannot be considered as rotationally symmetric.

In the Figure 6, the averaged measurements are compared with the results of the analytical and numerical models. On the left side the displacements are plotted over the radius and on the right side over the applied potential.
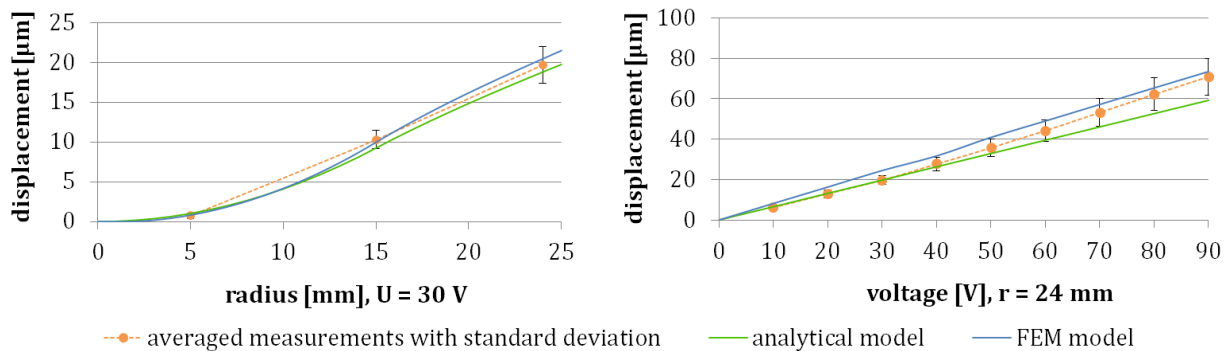
Figure 6: Comparison between analytical, numerical and experimental results

Both models are capable of reproducing the average displacements within the boundaries of the measured standard deviation.

5. VIBRATION MODES OF THE ACUTATOR: FEM AND EXPERIMENT

Using the described FE model, the first 27 normal modes of the actuator were obtained and for eleven of these solutions, corresponding measurement results were found. The comparison between the numerical results and the measurements is given in Figure 7, sorted by the frequency of the numerical solutions. The used measuring configuration to display the mode shapes is explained in Section 6. Since the number of possible measurements was limited due to practical reasons, it is possible that some of the other 14 mode shapes also occur with the real actuator but simply were not observed.

The results show that the model can be used to simulate the actuators behaviour with good approximation. For frequencies above 1000 Hz the model seems to be stiffer than the real actuators since the corresponding frequencies are considerably higher. But the data set of two actuators may be too small in order to make a statement. Comparing the two actuators, it can be seen that even equivalent actuators show huge differences for the frequencies of the individual vibration modes with a local maximum of the deflection.
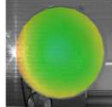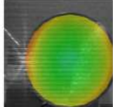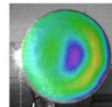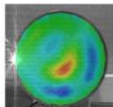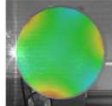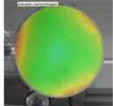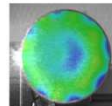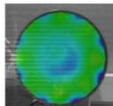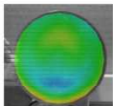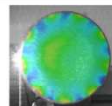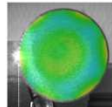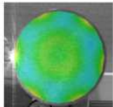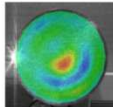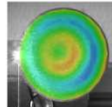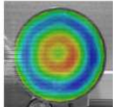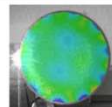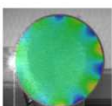
Figure 7: Comparison between numerical and measured normal modes

6. MEASUREMENT OF DYNAMIC DISPLACEMENT

The dynamic behaviours of the piezoelectric actuators were studied. Knowledge about the actuators natural modes can be useful for an energy-efficient usage e.g. in mobile robots. A large displacement can be achieved with minimal energy input. To analyse the vibration modes quantitatively, the Laser Doppler Vibrometer (LDV) *PSV-300* made by the *POLYTEC GmbH* was used. The measuring configuration can be seen in Figure 8 a). A function generator and a PC for data analysis are part of the *PSV-300* system. The function generator was used to generate sinusoidal signals with frequencies up to 20 kHz with the amplitude of 2 V. This signal was then amplified to 24 V and used to excite the piezoelectric actuator. The actuator was fixed the same way as for the static displacement measurements. With the LDV, only one point can be measured at a time which is why many sequential measurements have to be done. The individual measurements were synchronized using the excitation signal as a trigger. In Figure 8 b) the net consisting of about 400 measuring points is overlaid on the piezoelectric actuator. The intermediate areas were interpolated using the *PSV-300* software.
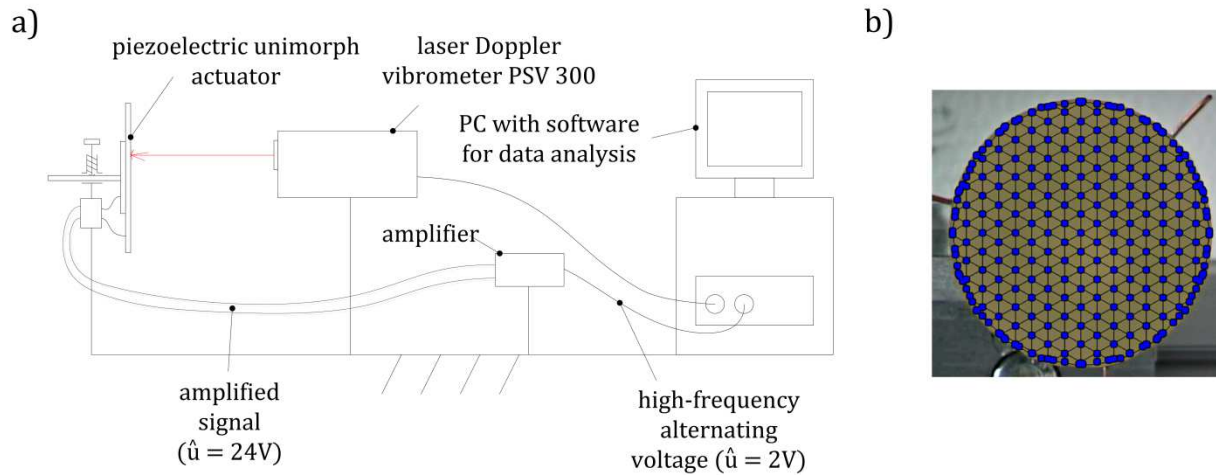

Figure 8: a) Configuration for measuring the dynamic displacement b) Distribution of measuring points along the surface

To determine the influence of different boundary condition, as they are present in the robots described in [1] and [2], to the vibration modes, three comparisons were made. At first, two equivalent piezoelectric actuators were compared to show differences that result from manufacturing tolerances. After that, three 50 mm long legs, like the ones used for piezoelectric driven micro robots, are attached to the actuator and the results are compared to the same actuator without legs. In a final comparison, the three legs were brought into contact with a glass surface and the results were compared to the actuator with free legs.

6.1 Comparison between two equivalent piezoelectric actuators
In Figure 9, the averaged velocity amplitudes of two equivalent actuators are shown for frequencies up to 20 kHz. In this case the velocity was chosen over the displacement because with this representation, peaks are easier to identify. Because of the harmonic oscillation the displacement can be obtained with the correlation

$$\hat{x} = \frac{\hat{v}}{2\pi \cdot f},$$

where $\hat{x}$ is the displacement amplitude, $\hat{v}$ the velocity amplitude and f the frequency [6].

Figure 9 reveals both similarities and differences between the two actuators. While both curves show a peak at about 560 Hz, the peaks in the range between 4000 and 6000 Hz differ considerably. This is probably due to the production tolerances which were mentioned in Section 4.
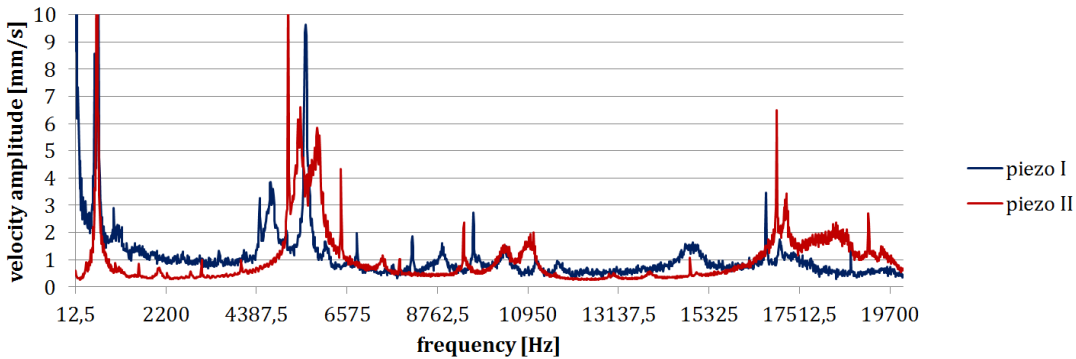

Figure 9: Averaged velocity amplitudes of two equivalent actuators for frequencies between 12.5Hz and 20,000Hz

After comparing the averaged velocity amplitudes, several frequencies were selected to measure the corresponding mode shapes. Figure 10 shows the mode shapes for three frequencies. At 563 Hz, both actuators vibrate in their first normal mode. The measured displacement of about 200 µm verifies that a resonant frequency since the static displacement for the used voltage was only 17 µm. The mode shapes for the other two frequencies differ significantly between both actuators.
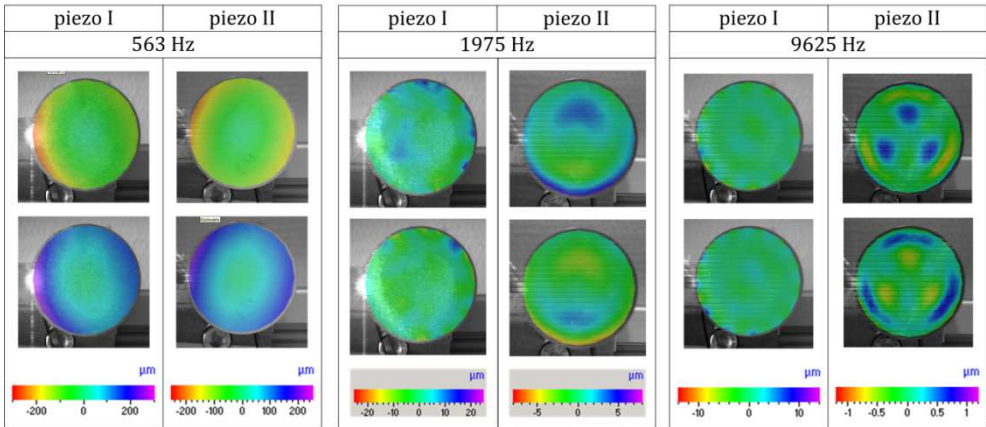

Figure 10: Mode shapes for two equivalent piezoelectric actuators

Figure 11 shows that similar mode shapes can be observed for different frequencies depending on the actuator.

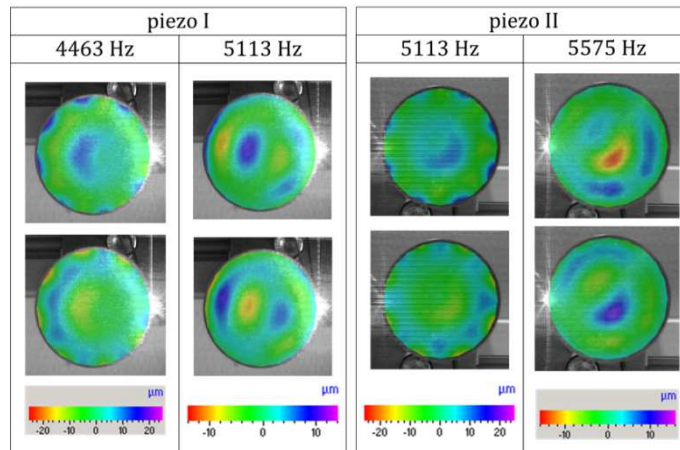| piezo I		piezo II	
4463 Hz	5113 Hz	5113 Hz	5575 Hz

Figure 11: Comparable mode shapes at different frequencies for two equivalent piezoelectric actuators

6.2 Comparison between a regular piezoelectric actuator and an actuator with attached legs

After comparing two equivalent actuators, three 50 mm long legs were radially soldered onto piezo II and the measurements were repeated. For this experiment, the legs were not brought in contact with a surface but could vibrate freely in the air. The averaged velocity amplitudes for both configurations are displayed in Figure 12. The differences suggest that the vibration behaviour is influenced by the additional legs.
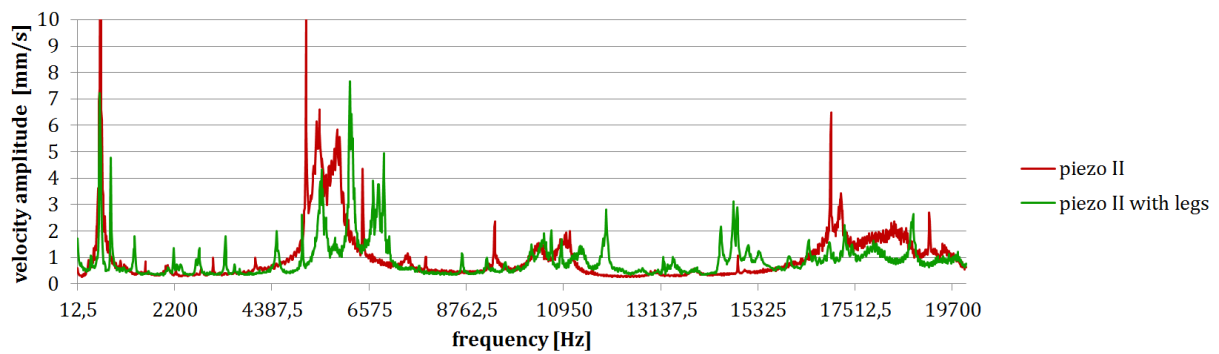

Figure 12: Averaged velocity amplitudes of a regular piezoelectric actuator and an actuator with attached legs for frequencies between 12.5 Hz and 20,000 Hz

In Figure 13, the mode shapes for three different frequencies are compared. Although there still is a peak at 560 Hz for both configurations, the mode shape for this frequency has changed significantly. The mode shapes for the other two frequencies seem similar in general. But it can be observed that the displacement amplitudes are considerably smaller at the points where the legs (marked with red lines) are attached to the brass plate. In conclusion, it can be noted that attaching legs to a piezoelectric actuator changes the vibration behaviour significantly.
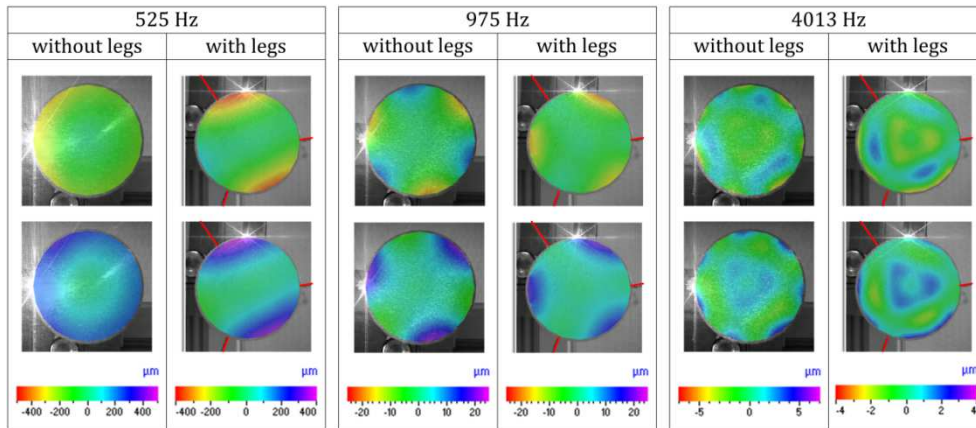
Figure 13: Mode shapes of a regular piezoelectric-actuator and an actuator with attached legs

6.3 Comparison between a piezoelectric-actuator with legs and an actuators with legs which are in contact with a glass surface

In a last comparison, the legs were brought into contact with a glass surface and the vibration behaviour was compared with the previous configuration. This was made to model the real constraints of a piezoelectric driven micro robot. The averaged velocity amplitudes are displayed in Figure 14. It can be seen that both curves are very similar.
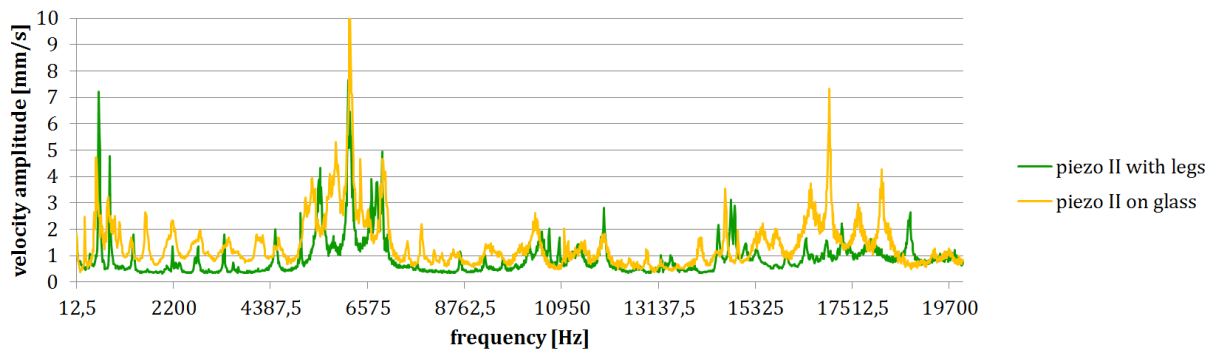

Figure 14: Averaged velocity amplitudes of a regular piezoelectric-actuator and an actuator with attached legs for frequencies between 12.5Hz and 20,000Hz

This observation was confirmed with the mode shapes for several frequencies. A sample of three comparisons can be seen in Figure 15. Most of the analysed mode shapes were very similar and not influenced by the contact with the glass surface.
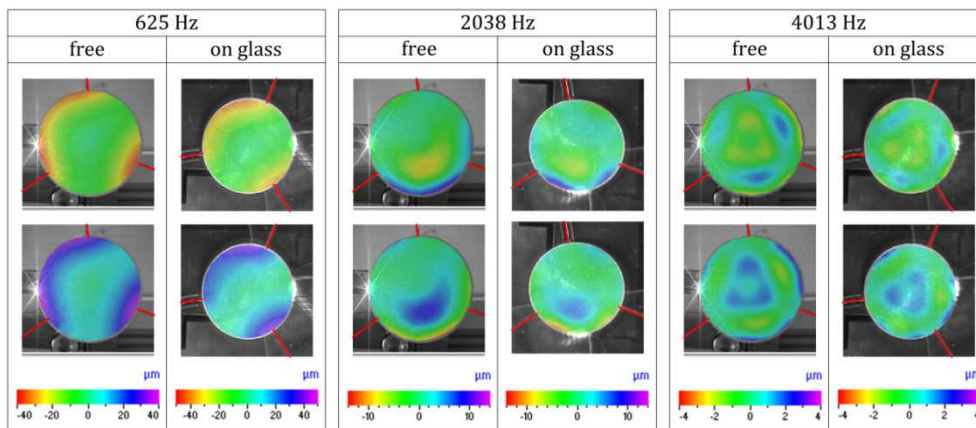

Figure 15: Mode shapes of a piezoelectric-actuator with attached legs and an actuator with attached legs which are in contact with a glass surface

7. CONCLUSIONS

It can be concluded that the studied piezoelectric low-cost unimorphs can be used as vibration actuators in the considered frequency range. The experimental results show that the value of the static deflection and the vibration modes for given frequencies differ considerably due to manufacturing tolerances. For the prototypes discussed in [1] and [2] this behaviour is critical. The possibility of a robot design with a priori defined frequency dependent locomotion behaviour is limited. Anyway fast and cheap robots can be created with the studied actuators. The relation between excitation frequency and motion of the robot needs to be obtained individually for each robot. The analytical and numerical results of the static deflection agree with the experiments.

REFERENCES

[1] F. Becker, V. Minchenya, K. Zimmermann, I. Zeidis, "Single Piezo Actuator Driven Micro Robot for 2-Dimensional Locomotion," Micromechanics and Microactuators, Vol. 2 of Mechanisms and Machine Science, Springer, Netherlands, pp 1–10, 2012.

[2] F. Becker, K. Zimmermann, T. Volkova, V. T. Minchenya, "An amphibious vibration-driven microrobot with a piezoelectric actuator," Regular and chaotic dynamics, Springer, Moscow, Vol. 18, 1/2, pp. 63-74, 2013.

[3] G. Pfeifer, "Piezoelektrische lineare Stellantriebe, " Wissenschaftliche Schriftenreihe der Technischen Hochschule Karl-Marx-Stadt, Bd. 6, 1982.

[4] I. Szabó, "Höhere technische Mechanik: nach Vorlesungen," 4. Aufl., Springer, Berlin, 1964.

[5] R. M. Jones, "Mechanics of composite materials," Taylor and Francis, Inc., Philadelphia 1999.

[6] Polytec GmbH, „Hardware Manual Polytec Scanning Vibrometer PSV-300", 2000.

CONTACTS

Dipl.-Ing. F. Becker	felix.becker@tu-ilmenau.de
B.Sc. S. Börner	simon.boerner@tu-ilmenau.de
B.Sc. E. James	emmanuel.james@tu-ilmenau.de
Prof. Dr. V. Minchenya	vlad_minch@mail.ru
Univ.-Prof. Dr.-Ing. habil. K. Zimmermann	klaus.zimmermann@tu-ilmenau.de